International Journal of Solids and Structures 49 (2012) 1852–1863

Contents lists available at SciVerse ScienceDirect

International Journal of Solids and Structures

journal homepage: www.elsevier.com/locate/ijsolstr

Determination of the interfacial properties of carbon nanotube reinforced polymer composites using atomistic-based continuum model

J.M. Wernik, B.J. Cornwell-Mott, S.A. Meguid *

Mechanics and Aerospace Design Laboratory, Department of Mechanical and Industrial Engineering, University of Toronto, 5 King's College Road, Toronto, Ontario, Canada M5S 3G8

ARTICLE INFO

Article history:
Received 13 April 2011
Received in revised form 7 February 2012
Available online 30 March 2012

Keywords:
Carbon nanotube reinforced polymer composites
Interfacial properties
Atomistic-based continuum
Multiscale modeling
Nanotube pull-out

ABSTRACT

The present study investigates the interfacial properties of carbon nanotube (CNT) reinforced polymer composites by simulating a nanotube pull-out experiment. An atomistic description of the problem is achieved by implementing constitutive relations that are derived solely from interatomic potentials. Specifically, we adopt the Lennard-Jones (LJ) interatomic potential to simulate a non-bonded interface, where only the van der Waals (vdW) interactions between the CNT and surrounding polymer matrix are assumed to exist. The effects of such parameters as the CNT embedded length, the number of vdW interactions, the thickness of the interface, the CNT diameter and the cut-off distance of the LJ potential on the interfacial shear strength (ISS) are investigated and discussed. The problem is formulated for both a generic thermoset polymer and a specific two-component epoxy based on a diglycidyl ether of bisphenol A (DGEBA) and triethylene tetramine (TETA) formulation. The study further illustrates that by accounting for different CNT capping scenarios and polymer morphologies around the embedded end of the CNT, the qualitative correlation between simulation and experimental pull-out profiles can be improved.

1. Introduction

Since their discovery by Iijima (1991), CNTs have been the subject of immense research; primarily because of their remarkable properties which include their miniature size, high aspect ratio, low density, high strength and high stiffness. The exceptional mechanical properties of CNTs have shown great promise for a wide variety of applications, such as nanotransistors, semiconductors, hydrogen storage devices, structural materials, molecular sensors, field-emission based displays, and fuel cells, to name a few (Endo et al., 2004). Apart from the abovementioned applications, CNTs have also been introduced as reinforcing agents in lightweight polymeric composite materials. It has been recognized for some time that the mechanical, thermal and electrical properties of polymeric materials can be engineered by fabricating composites that are comprised of different volume fractions of one or more reinforcing phases. Traditionally, polymeric materials have been reinforced with carbon or glass microfibres to improve their mechanical properties and a variety of metallic and/or organic fillers for electrical and thermal property enhancements. These composite materials have been used in a wide variety of applications in automotive, aerospace, mass transit, and nuclear industries. As time has progressed, practical realization of such composites has begun to shift from micro-scale composites to nanocomposites, taking advantage of the unique combination of mechanical, electrical and thermal properties of *nanofillers* (fillers with a characteristic dimension below 100 nm). There are three main advantages associated with dispersing nano-scaled fillers, such as CNTs, in polymeric materials. They are the phenomenal mechanical, electrical and thermal conductivities, nanoscopic size and their high aspect ratios. Whilst some credit can be attributed to the intrinsic properties of the nanotubes, most of these advantages stem from the extreme reduction in filler size combined with the large enhancement in the specific surface area and interfacial area they present to the matrix phase.

The mechanical properties of a composite material are governed by the characteristics of the reinforcing filler-polymer matrix interface. The interface is largely responsible for stress transfer from the surrounding matrix to the reinforcement. As such, the extremely high aspect ratios of CNTs lend themselves to greatly improved transferability of load at the interface, when compared with conventional microfibers. However, the degree of interfacial adhesion between the nanotubes and polymer also becomes a key parameter affecting the physical properties of the nanoreinforced composite. The carbon atoms on CNT walls are chemically stable because of the aromatic nature of the bonding. As a result, the reinforcing CNTs interact with the surrounding polymer matrix mainly through weak van der Waals interactions (Hu et al., 2006).

Earlier studies suggest that it is possible to improve the interfacial strength between the CNTs and polymer matrix using chemical

* Corresponding author. Tel.: +1 416 978 5741; fax: +1 416 978 7753.
E-mail address: meguid@mie.utoronto.ca (S.A. Meguid).

0020-7683/$ - see front matter © 2012 Elsevier Ltd. All rights reserved.
http://dx.doi.org/10.1016/j.ijsolstr.2012.03.024

modification techniques. These include both non-covalent and covalent functionalization of the CNTs. Non-covalent functionalization refers to the adsorption of surfactant molecules or the helical wrapping of polymer molecules on the CNT walls which in turn improves the wetting of the CNTs by the polymer. Covalent functionalization or chemical cross-linking refers to the formation of a small percentage of strong covalent bonds between the CNT and surrounding polymer from the grafting of functional groups on the CNT walls. Experimental nanotube pull-out tests seem to support the idea that these mechanisms can increase the ISS of CNT polymer composite systems. For example, the work by Wagner's group has demonstrated that the ISS between a multiwalled carbon nanotube (MWCNT) and an epoxy matrix is in the range of 35–376 MPa using a scanning probe microscope (SPM) setup to drag the nanotube out from the matrix (Cooper et al., 2002). Later, they employed an atomic force microscope (AFM) to directly pull a MWCNT from a polyethylene-butene matrix and observed an average interfacial stress of 47 MPa (Barber et al., 2003). Traditional composite materials containing microfibre reinforcements embedded in thermoplastic matrices typically exhibit interfacial strengths below 10 MPa (Mader et al., 1996). Furthermore, computer simulations have shown that the interfacial strength of a CNT polyethylene system is on the order of 2 MPa, when only vdW interactions were considered (Frankland et al., 2002). Therefore, it can be concluded that some form of covalent bonding does naturally occur in the above system as evidenced by the high interfacial strength. An ISS as high as 500 MPa has been observed as reported by Wagner et al. (1998) based on fragmentation tests in urethane-CNT composites albeit assumptions made on both the critical length and nanotube strength. On a separate occasion, Wagner's group directly explored the effect of functionalization by using both pristine and chemically modified MWCNTs in their AFM experiments. The shear-lag fits give an average ISS of approximately 30 MPa in the case of pristine CNTs, and 151 MPa for the chemically modified nanotubes (Barber et al., 2006). In comparison, the theoretical findings of Zheng et al. (2009), using molecular dynamics (MD), report ISS of 33 MPa and approximately 575 MPa for cases involving pristine non-bonded nanotubes and phenyl functionalized nanotubes in a polyethylene matrix, respectively. Finally, the MD model of Xu et al. (2002) predicts an ISS of approximately 138 MPa when considering non-bonded interactions between a nanotube and epoxy matrix. Despite the promising improvements observed in the ISS, both functionalization techniques have been shown to compromise the intrinsic properties of CNTs by introducing structural changes or defects in the walls of the nanotube (Garg and Sinnott, 1998; Fiedler et al., 2006). This becomes especially detrimental when attempting to implement multifunctional capabilities in the composite. Structural defects can significantly alter the intrinsic properties of the nanotubes which can in turn result in a substantial degradation in the thermal and electrical conductivity of the composite and its mechanical performance.

Evidently, a number of analytical, numerical and experimental works has been done to help understand the complexities of the CNT polymer interface. However, correlation between these results is often difficult due to (i) significant variability in the materials, processing techniques and procedures that are employed in experimental studies and (ii) differences in the adopted simulation techniques and the way the pull-out problem is formulated in the numerical investigations. Some conclusions drawn experimentally have not been observed in numerical and analytical simulations. Specifically, experimental results exhibit high pull-out forces at the initial stage of the pull-out process. This is immediately followed by a sudden decay in the force until the CNT has fully been withdrawn from the polymer. On the contrary, the pull-out forces predicted by numerical simulations seem to increase to a relatively fixed value until the last stages of the pull-out process. Therefore, several fundamental differences between experimental studies and numerical simulations are worthy of investigation. In particular, little focus has been placed on the effect of CNT capping and the morphology of the polymer around the embedded tip of the CNT and the effect of CNT diameter. It is expected that if the polymer matrix fully embodies the embedded CNT, the additional vdW interactions at the base will serve to increase the initial pull-out force.

It is therefore necessary to re-examine the non-bonded van der Waals interaction mechanism and its key parameters to identify any potential processing techniques that can be implemented in order to improve the strength of the interface without resorting to a functionalization treatment and to better correlate the numerical predictions to experimentally observed pull-out profiles. Experimental measurements of the interfacial properties of CNT polymer composites are severely hindered by the length-scale involved when using CNTs. Therefore, an effective way of quantifying such properties is through the use of computational modeling techniques. This paper expands on the existing literature of CNT polymer interfaces and describes the development of a multiscale computational model used to investigate the interfacial properties of non-bonded CNT polymer systems. Specifically, the effect of the CNT embedded length, the thickness of the interface, the cut-off distance of the LJ potential and the number of vdW interactions considered is investigated. Furthermore, the effect of different CNT capping conditions and CNT diameters is also examined with the intent to better replicate the pull-out profiles observed experimentally.

2. Numerical approach

To investigate the interfacial properties of a CNT-polymer composite system a pull-out test of the nanotube is simulated. Fiber pull-out tests have been well recognized as the standard method for evaluating the interfacial bonding properties of composite materials. The output of these tests is the force required to pull-out the nanotube from the surrounding polymer matrix and the corresponding interfacial shear stresses involved. The problem is formulated using a representative volume element (RVE) which consists of the reinforcing CNT, the surrounding polymer matrix, and the CNT/polymer interface as depicted in Fig. 1(a). Fig. 1(b) shows a schematic of the pull-out process, where x is the pull-out distance and L is the embedded length of the nanotube. The atomistic-based continuum (ABC) multiscale modeling technique is used to model the RVE. The approach adopted here extends the earlier work of Wernik and Meguid (2011). The new features of the current work relate to the approach adopted in the modeling of the polymer matrix and the investigation of the CNT polymer interfacial properties as appose to the effective mechanical properties of the RVE. The idea behind the ABC technique is to incorporate atomistic interatomic potentials into a continuum framework. In this way, the interatomic potentials introduced in the model capture the underlying atomistic behaviour of the different phases considered. Thus, the influence of the nanophase is taken into account via appropriate atomistic constitutive formulations. Consequently, these measures are fundamentally different from those in the classical continuum theory. For the sake of completeness, we provide a brief outline of the method detailed in our earlier work (Wernik and Meguid, 2011).

The CNT is modeled as a space-frame structure as depicted in Fig. 2. In the space-frame model, each beam element corresponds to an individual chemical bond in the CNT. As in traditional FE models, nodes are used to connect the beam elements to form the CNT structure. In this case, the nodes represent the carbon

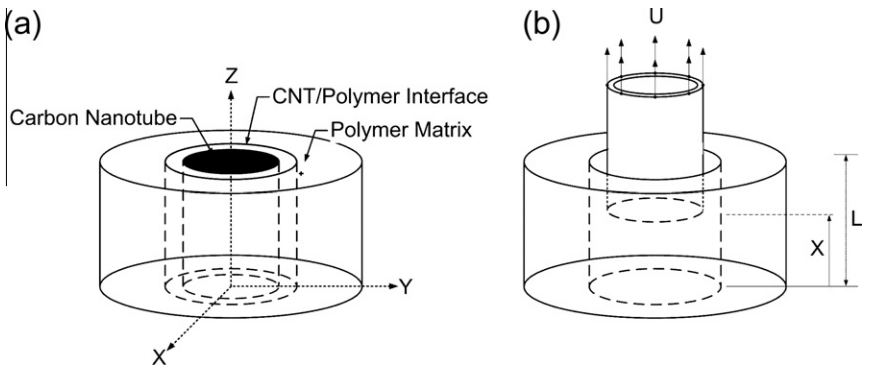

Fig. 1. Schematic depictions of (a) the representative volume element and (b) the pull-out process.

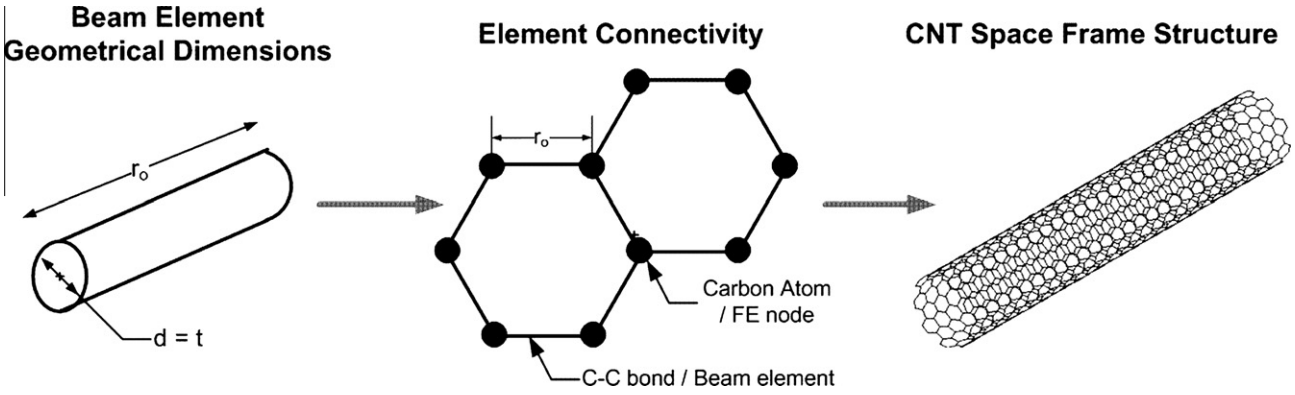

Fig. 2. Carbon nanotube geometrical space frame structure.

atoms and their positions are defined by the same atomic coordinates. Consequently, the terms node and atom are used interchangeably throughout this paper. We adopt the Modified Morse potential with an added angle-bending potential to describe the atomic interactions in the CNT. This potential is given by:

$$E = E_s + E_b \tag{1}$$

$$E_s = D_e([1 - \exp^{-\beta(r-ro)}]^2 - 1) \tag{2}$$

$$E_b = \tfrac{1}{2}k_\theta(\theta - \theta_o)^2[1 + k_{sextic}(\theta - \theta_o)^4] \tag{3}$$

where r_o is the initial bond length, θ_o is the initial angle between adjacent bonds, D_e is the dissociation energy, β is a constant which controls the 'width' of the potential, and k_θ and k_{sextic} are the angle-bending force constants. The parameters used for the potential in this study were the same as those adopted by Belytschko et al. (2002), and are presented in Table 1. Nonlinear rotational spring elements are used to account for the angle-bending component, while beam elements are used to represent the stretching component of the potential. Differentiating the stretching potential (Eq. (2)) with respect to the change in bond length and by utilizing the following relationship, $\varepsilon = (r - ro)/ro$, we can arrive at the expression:

$$F = 2\beta D_e(1 - \exp^{-\beta\varepsilon r_o})\exp^{-\beta\varepsilon r_o} \tag{4}$$

which represents the force required to stretch a C–C bond. This expression is used to describe the material behavior of the beam elements. Likewise, differentiating the angle-bending component of the potential Eq. (3)) with respect to the change in rotation, we can arrive at the following expression:

$$M = k_\theta(\theta - \theta_o)[1 + 3k_{sextic}(\theta - \theta_o)^4] \tag{5}$$

which represents the moment required to bend neighboring bonds. Again, this expression is used to define the stiffness of the rotational spring elements throughout the simulation.

The Lennard-Jones interatomic potential is used to describe the vdWs interactions at the CNT/polymer interface. The LJ potential is defined as

$$E_{LJ} = 4\mu\left[\left(\frac{\psi}{r}\right)^{12} - \left(\frac{\psi}{r}\right)^{6}\right] \tag{6}$$

where μ is the potential well depth, ψ is the hard sphere radius of the atom or the distance at which E_{LJ} is zero, and r is the distance between the two atoms. In this study, we investigate the non-bonded interactions between the carbon atoms in the CNT and the atoms in the polymer. The LJ parameters for the interactions considered in this paper are summarized in Table 2. Again, by differentiating the potential with respect to the separation distance, we arrive at an expression for the vdW force between two interacting atoms

$$F_{LJ} = 24\left(\frac{\mu}{\psi}\right)\left[2\left(\frac{\psi}{r}\right)^{13} - \left(\frac{\psi}{r}\right)^{7}\right] \tag{7}$$

Table 1
Modified Morse potential parameters.

Parameter	Value
r_o (m)	1.421×10^{-10}
D_e (N m)	6.03105×10^{-19}
B (m^{-1})	2.625×10^{10}
θ_o (rad)	2.094
k_θ (N m rad^{-2})	0.876×10^{-18}
k_{sextic} (rad^{-4})	0.754

Table 2
Lennard-Jones potential parameters.

LJ interaction	μ (J)	ψ (nm)
Carbon–carbon (C–C)	3.89×10^{-22}	0.34
Carbon–hydrogen (C–H)	4.44×10^{-22}	0.32
Carbon–oxygen (C–O)	4.90×10^{-22}	0.32
Carbon–nitrogen (C–N)	4.48×10^{-22}	0.33

This expression is used to determine the magnitude of the force in each interaction, which depends solely on the separation distance between the atoms and the type of atoms considered. Each carbon atom in the CNT is involved in an enormous number of vdW interactions with the atoms in its surroundings. Therefore, to avoid excessive computational costs, no additional finite elements are included in the interface description, as was done in our earlier work where each interaction was represented by its individual finite element. Alternatively, the cumulative effect of the vdW interactions acting on each CNT atom is applied as a resultant force on the respective node which is then resolved into its three Cartesian components. This process is depicted in Fig. 3. During each iteration of the pull-out process, the above expression is re-evaluated for each vdW interaction and the cumulative resultant force and its three Cartesian components are updated to correspond to the latest pull-out configuration. Fig. 4 shows a segment of the CNT with the cumulative resultant vdW force vectors as they are applied to the CNT atoms.

In the present study, we consider both a generic thermoset polymer and a specific two-component epoxy system. The generic polymer system will allow for us to identify the effect of polymer morphology and atomic density in the region surrounding a CNT on the ISS. Variations in polymer morphology and atomic density can also be interpreted as a means of investigating the effect of the number of vdW interactions considered. In this case, the polymer atoms involved in the vdW interactions at the interface are modeled as rings of nodes forming concentric cylinders around the CNT space-frame structure. This approach adopts ordered and uniformly distributed representative nodes of the polymer structure. In the case of the two-component epoxy system, the representative nodes are randomly distributed throughout a constant volume surrounding the CNT. We feel that this approach will provide a much more realistic depiction of the polymer and allow for us to predict the ISS for a specific CNT polymer system. In both cases we consider the vdW interactions between the nanotube and the inner surface of the polymer matrix as well as those which extend further into the immediate surrounding matrix. It is expected that cured thermoset polymer systems of a highly cross-linked formulation would show little deformation in the region surrounding a nanotube during a pull-out experiment. Therefore, the representative nodes of the polymer are fully constrained and primarily serve to provide the coordinates of the polymer atoms involved in the vdW force evaluation procedure described above. The nodes in the CNT are constrained from any radial displacements and an incremental axial displacement boundary condition is applied to the top CNT nodes to initiate the pull-out process. The displacement boundary conditions are summarized in Fig. 5.

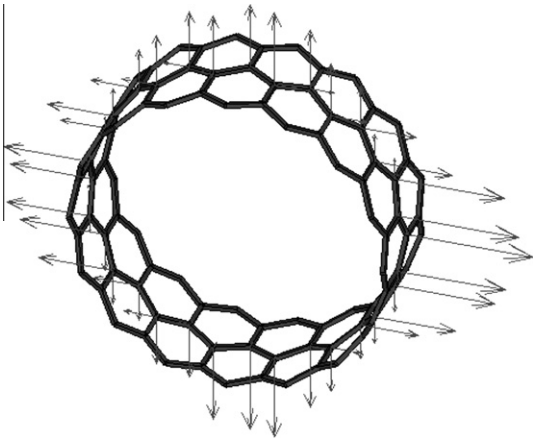

Fig. 4. Segment of CNT with cumulative resultant vdW force vectors.

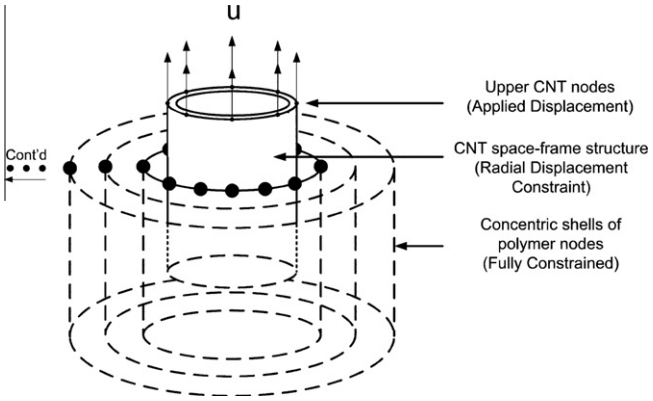

Fig. 5. Polymer representation and pull-out boundary conditions.

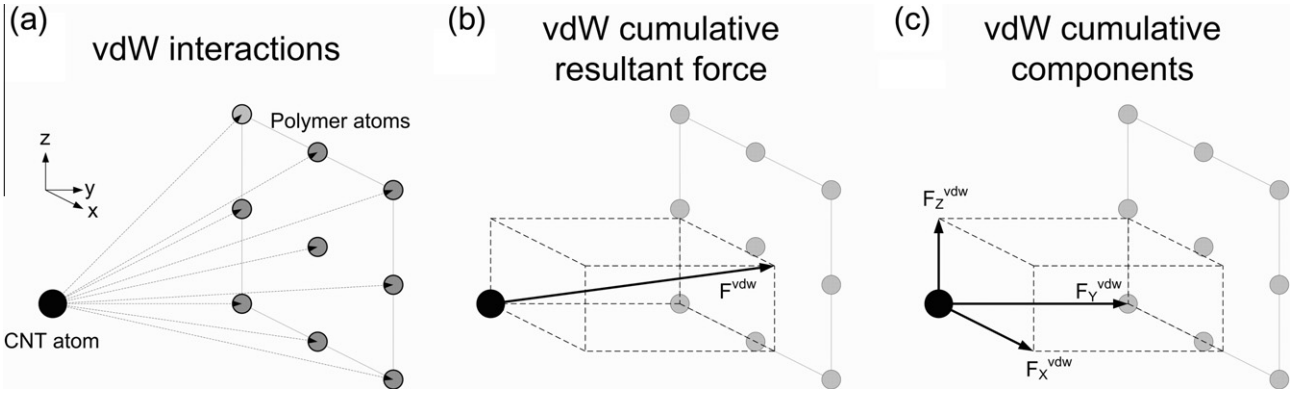

Fig. 3. The process of nodal vdW force application. (a) vdW interactions on an individual CNT atom, (b) the cumulative resultant vdW force, and (c) the cumulative vdW Cartesian components.

3. Results and discussion

The present study uses a representative volume element to investigate the interfacial properties of the CNT polymer composite system. The force required to withdraw the CNT from the matrix is evaluated over the course of the pull-out process by summing the reaction forces at the upper CNT nodes. The corresponding ISS can then be calculated by dividing the maximum pull-out force by the initial interfacial area, $A = \pi dl$, where d and l are the diameter and length of the embedded nanotube, respectively. Fig. 6 depicts a simulated pull-out profile (pull-out force vs. pull-out distance) for the generic polymer system. After an initial loading segment, a sliding or steady state regime ensues as the nanotube is gradually pulled through the surrounding matrix. The pull-out force then decreases as the end of the CNT approaches the upper surface of the polymer matrix. One can observe that the pull-out force exhibits relatively little variation in the sliding regime. However, this is not a common characteristic of all predicted pull-out profiles. Rather the smoothness of the sliding regime is due to a high polymer nodal density and the ordered and uniformly distributed polymer nodal representation. In this generic study, the interface region is saturated with a high number of vdW interactions which prevents any sharp oscillations in the pull-out force as the CNT is withdrawn from the matrix. It is worth noting that the work also included the effect of random distribution of the polymer atoms, as explained later on, and this will result in sharp peaks and valleys in the pull-out profile which correspond regions of high and low vdW interactions during the respective pull-out process. The general pull-out profile depicted in Fig. 6 shows striking resemblance with those obtained by Xia and Curtin (2004) in their MD studies of the sliding behavior of MWCNTs. This MWCNT "sword-and-sheath" deformation can also be viewed as a composite system wherein the outer walls represent a matrix material surrounding a broken nanotube. In comparison, pull-out profiles obtained experimentally via the direct tensile loading of the CNT using an AFM setup do show discrepancies. For example, the results of Barber et al. (2003) show an initial rise in the pull-out force until a critical force is reached at which point the interface is thought to have failed and a large drop in the force is subsequently observed with no evidence of a sliding regime (Fig. 7(a)). A similar profile is observed in the experimental results of Cooper et al. (2002) using a SEM setup (Fig. 7(b)). These discrepancies can be explained as follows. The present study treats the CNT as a continuous fibre that extends the same distance as the surrounding matrix in the RVE. As such, it does not take into account the end effects that may result from the capping of the CNT and the added vdW interactions that would occur if the base of the CNT were also embedded in the polymer. These end effects would significantly increase the peak pull-out force during the initial stages of loading as will be shown in Section 3.6 of the present article.

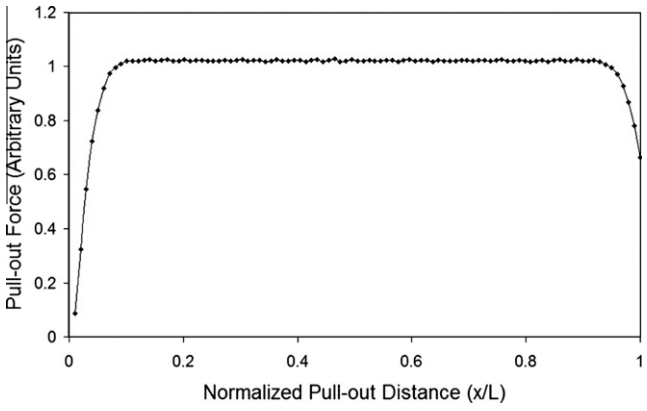

Fig. 6. Typical CNT pull-out profile.

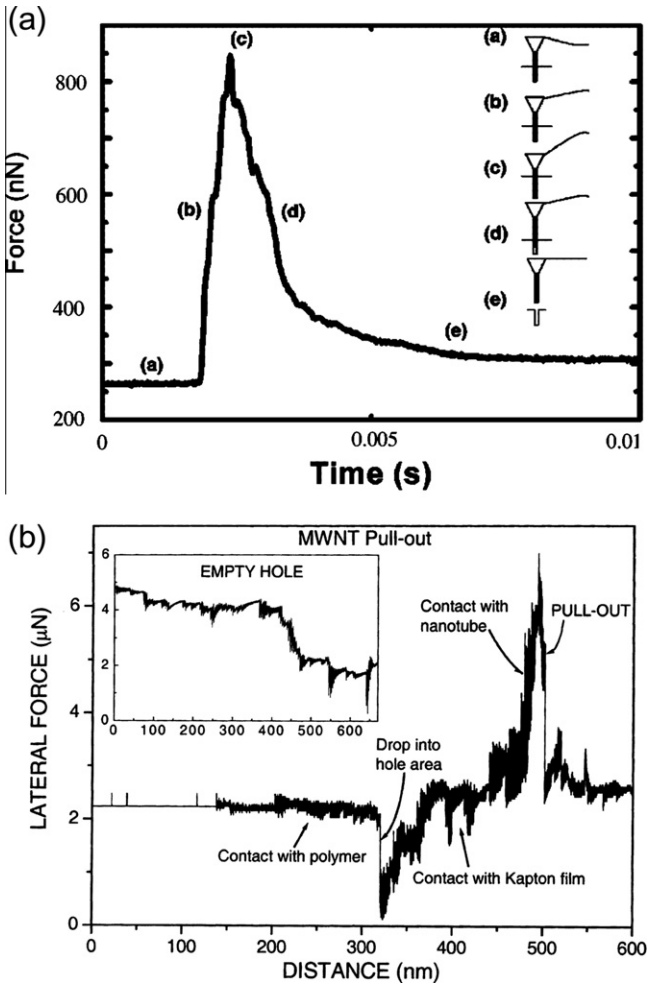

Fig. 7. Experimental pull-out profiles using an (a) AFM (after [5]) and (b) SEM setup (after [4]).

The discrepancies between experimentally observed and simulated profiles can also be explained by the time scale over which the pull-out process occurs. Once the interface has failed, the subsequent sliding of the nanotube occurs rapidly. It is believed that experimental techniques are hindered by the temporal resolution of the equipment used and are incapable of attaining sufficient measurements to capture this sliding regime. Furthermore, the experimental works are unable to ensure a perfect non-bonded system as the one investigated in the present work. As a result, the CNT polymer system considered in these works may in fact have a degree of functionalization present which could explain the sharp peak evident in their pull-out profiles.

3.1. Effect of van der Waals interactions

Atomistic simulations, such as MD, can be used to determine the exact morphology of a polymer system surrounding a nanotube structure. Without first employing MD simulations to determine the exact morphology of the polymer chains in their lowest energy state, it is rather difficult to establish the exact location of the atoms in the near vicinity of the CNT. However, MD results can show significant variability depending on the potentials used, the polymer system being investigated, the chosen timestep algorithm, and how the boundary conditions are applied. In this study, the

polymer matrix is represented by a series of nodes forming concentric cylinders around the reinforcing nanotube space-frame structure (Fig. 5). We feel that this description forms an adequate basis on which the interfacial properties of a generic polymer CNT system can be investigated. The density of nodes in the polymer description will determine the number of vdW interactions between the CNT and the surrounding polymer, and consequently, the resulting ISS. To study the sensitivity of this parameter on the ISS, the number of nodes in the polymer representation is varied. Three studies are conducted to investigate the effect of polymer atomic density, or equivalently, the number of vdW interactions. In each study, a CNT of 1.776 nm in length and an interfacial thickness of 0.34 nm is used. The first study considers only the immediate surrounding layer of the polymer and varies its number of nodes (Fig. 8(a)). In the second study, the number of nodes in the polymer layers remain constant but the number of layers surrounding the CNT is increased using an interlayer spacing of 0.1275 nm (Fig. 8(b)). This interlayer spacing was selected to ensure a uniform distribution of the nodes throughout the polymer volume. The third study utilizes a computational cell of constant volume that extends 1.0 nm into the surrounding polymer (Fig. 8(c)). This study considers variations in the proximity of the layers and the number of vdW interactions are varied by increasing the number of layers in the defined volume. In all three studies, the chemical composition of the polymer is ignored, implying that only carbon-carbon vdW interactions are considered.

Four interfacial configurations are considered in Study 1 with vdW interaction densities (δ) corresponding to 5000, 10,000, 19,000 and 37,000 vdW interactions per square nanometer CNT (int/nm^2), respectively. The vdW interaction density represents the total number of vdW interactions occurring during the pull-out process divided by the surface area of the nanotube. Fig. 9 shows the predicted linear dependency of the ISS on the vdW interaction density for the case where only the immediate surrounding layer of the polymer was considered. Fig. 10 shows the effect of vdW interaction density on the ISS for studies 2 and 3. In both studies the ISS increases with increasing number of layers and interaction density. However, in study 2 the number of layers considered does not seem to have a significant effect beyond the fourth layer. This study used a constant interlayer spacing and successively added more layers to the surrounding polymer. The ISS begins to plateau because as more layers are added, the atoms are situated at a further distance from the CNT. The corresponding vdW interactions become weaker due to the large atomic separation distance. For example, the fifth layer is situated at a radial distance of 0.85 nm from the wall of the CNT. This distance also corresponds to the traditional LJ cut-off distance used in MD simulations where the potential is truncated to ignore interactions that extend beyond this distance. Study 3, however, does show a continually increasing ISS with increasing number of layers and

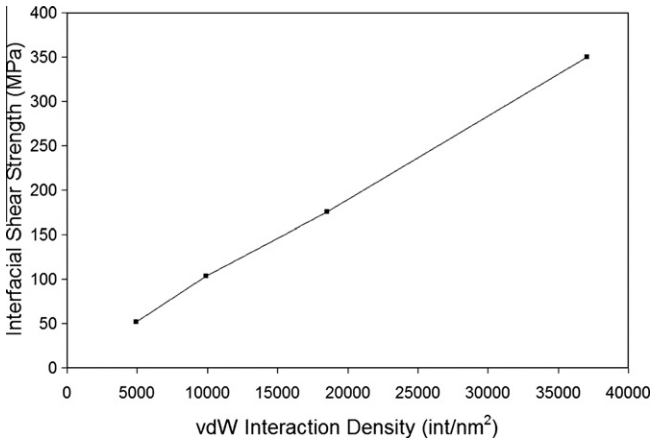

Fig. 9. The effect of the vdW interaction density on the interfacial shear strength when only inside surface of polymer is considered.

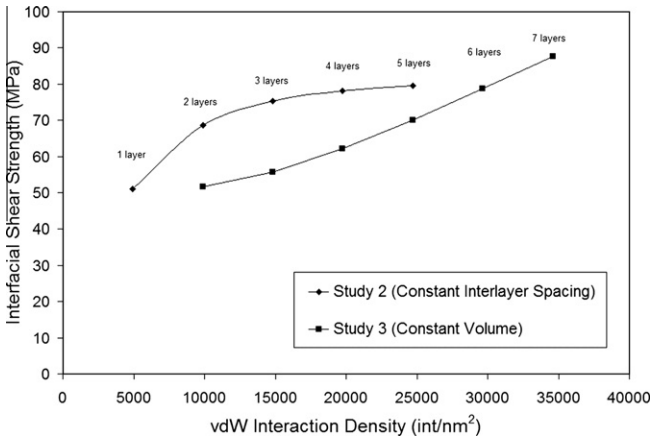

Fig. 10. The effect of the vdW interaction density on the interfacial shear strength when multiple polymer layers are considered.

interaction density. This study used a computational cell of constant volume. As more layers are added to the cell their interlayer spacing decreases. This also shifts some of the atoms to within a closer distance of the CNT resulting in stronger vdW interactions thus increasing the ISS. The trend observed in study 3 seems to exhibit a similar linear dependence as in study 1.

The above three studies can be used to help identify the effect of polymer morphology and atomic density in the region surrounding a CNT on the ISS of a generic polymer CNT system. However, one cannot extrapolate a value from these results for a specific polymer

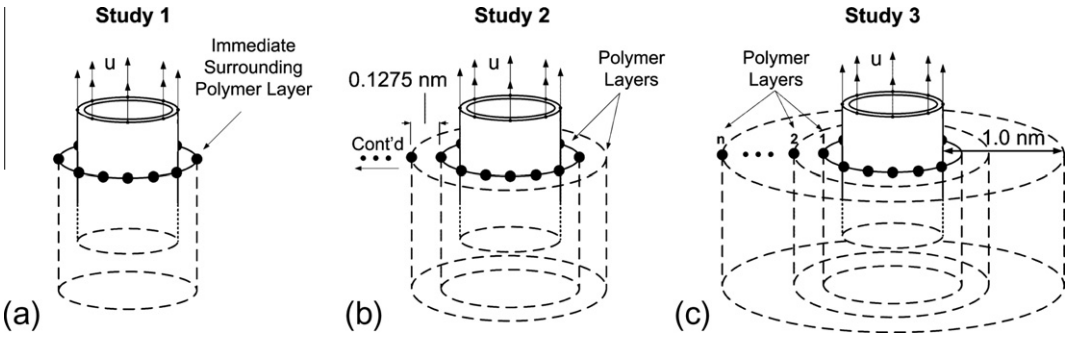

Fig. 8. Schematic diagram of polymer representations used to study the effect of vdW interaction density using (a) only the inside polymer surface (Study 1), (b) multiple polymer layers with a constant interlayer spacing (Study 2), and (c) a constant volume with varied interlayer spacings (Study 3).

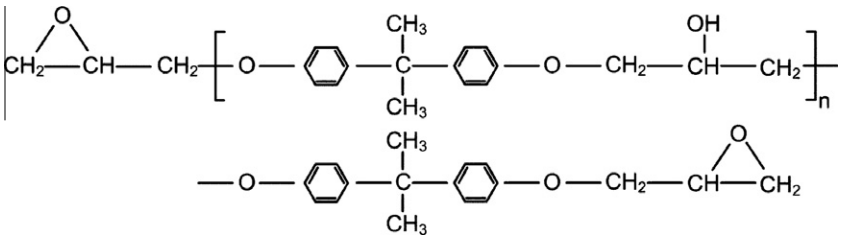

Fig. 11. Atomic structure of diglycidyl ether of bisphenol A (DGEBA) base resin.

system. For the sake of completeness the authors present a final study for which a reasonable estimate of the ISS of a specific two-component epoxy polymer CNT system is predicted. This system is used as the computational model for the remaining analyses of this paper. A simple epoxy resin, based on diglycidyl ether of bisphenol A (DGEBA) and a common curing agent, triethylene tetramine (TETA), is selected.

To determine the number of vdW interactions between the CNT and atoms of the surrounding epoxy matrix, the atomic density of the two-component epoxy system is determined using simple stoichiometric calculations. The base resin exhibits the atomic structure depicted in Fig. 11, where '*n*' is approximately 0.15. This atomic structure corresponds to a molecular mass of approximately 383.07 g/mol, with a molecular formula of $C_{23.7}H_{27}O_{4.5}$. The density of the resin is 1.16 g/cm^3. The atomic structure of the curing agent is depicted in Fig. 12. It has a corresponding molecular mass of 146.23 g/mol, with a molecular formula of $C_6H_{18}N_4$ and a density of 0.93 g/cm^3. The mix ratio between the base resin and curing agent is 100 parts to 12.9 parts, respectively. Therefore a sample of the cured epoxy would have a density of approximately 1.09 g/cm^3, with an average polymer chain composed of $C_{21.67}H_{26}O_4N_{0.45}$. This corresponds to an average polymer chain mass of 356.01 u (atomic mass units), or 5.912×10^{-22} g. From this, a molecular density of 1.843×10^{21} mol/cm^3, or 1.843 mol/nm^3, can be derived. Based on the above calculations, the approximate quantities of atoms present in the surrounding matrix (per cubic nanometre) are determined and provided in Table 3.

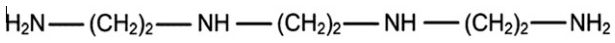

Fig. 12. Atomic structure of triethylene tetramine (TETA) curing agent.

Table 3
Approximate quantities of atoms present in the surrounding matrix per cubic nanometer.

Element	Atoms/nm^3	% of Total
Carbon (C)	39.87	42 %
Hydrogen (H)	47.84	50 %
Oxygen (O)	7.36	7 %
Nitrogen (N)	0.83	1 %

From this, we can infer an approximate *polymer nodal density* of 96 nodes/nm^3. For the present study, we adopt a constant volume of polymer surrounding the CNT that extends a radial distance of 1.00 nm from the wall of the CNT. The model also utilizes an interfacial thickness of 0.34 nm and a CNT of 6.60 nm in length. The surrounding polymer has a volume of 35.49 nm^3 which corresponds to a total of 3407 polymer nodes and a total of 3,379,744 vdW interactions occurring during the pull-out process. The polymer nodes are randomly distributed throughout this volume. In this way, the polymer representation closely mimics that of a true polymer system whereby the polymer chains adopt a random configuration. Fig. 13 depicts the CNT embedded in the random two-component epoxy system and the distribution of polymer nodes. Using the procedure outlined above the ISS for the present two-component epoxy system of 6.60 nm in length is predicted to be 21.98 MPa and the corresponding pull-out profile is depicted in Fig. 14. In comparison, Zheng et al. (2009) predicted a non-bonded ISS of approximately 33 MPa for a CNT of 5.9 nm in length embedded in a polyethylene matrix via MD. The results are comparable and any discrepancies can be attributed to differences in the CNT diameter and the different polymer systems investigated.

It should be noted that the predicted polymer nodal density is only a rough estimate and is based on a number of key assumptions. For example, the above approach assumes that there are no significant secondary reactions or by-products forming during the curing process that would drastically change the average polymer composition or density. The stochastic nature of epoxies means that the density of atoms will vary, depending on how the resin and hardener interact and the curing temperature. Also, in a practical setting, the atomic density will change depending on what other constituents are mixed into the resin or hardener, and what anomalies or voids are introduced during the manufacturing of the nanocomposite. Even the most sophisticated methods

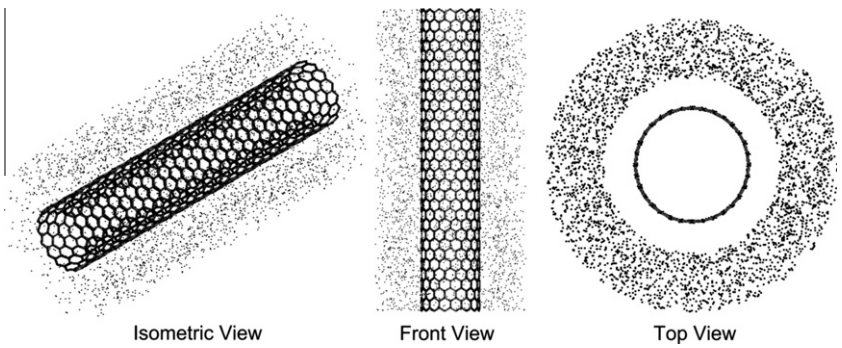

Fig. 13. CNT embedded in random polymer nodal distribution.

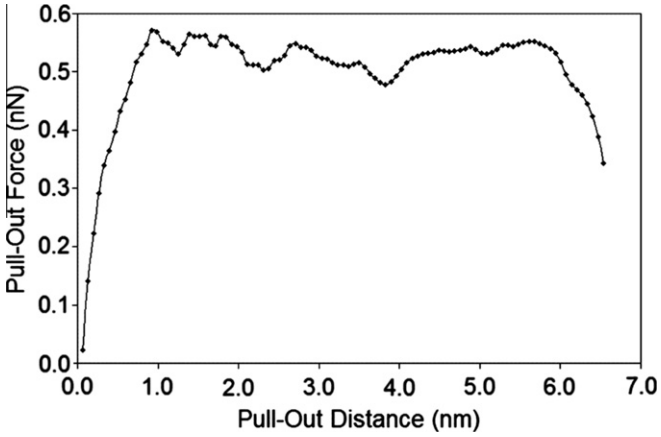

Fig. 14. Pull-out profile for CNT embedded in DGEBA/TETA two-component epoxy system.

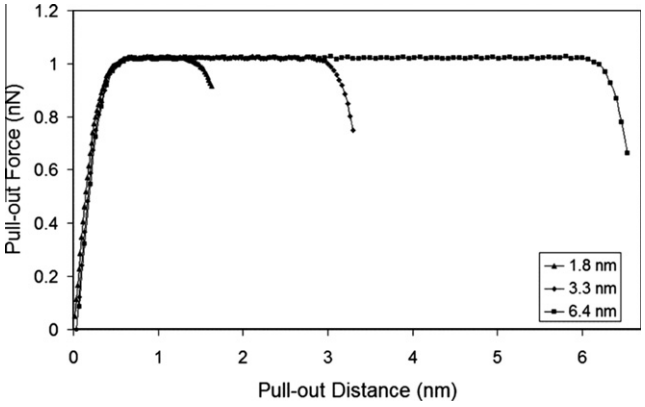

Fig. 16. Pull-out profiles for CNTs with different embedded lengths in the generalized polymer formulation.

of determining atomic density (such as MD simulations) would fail to account for all the possible variations.

3.2. Effect of CNT embedded length

Fig. 15 shows simulated pull-out profiles for nanotubes of three different lengths; 3.3 nm, 6.6 nm, and 12.8 nm with an interfacial thickness of 0.34 nm. At first glance one may conclude that the maximum pull-out force increases with embedded CNT length, particularly when comparing the 6.6 and 12.8 nm profiles. However, the additional sharp peaks evident in the 12.8 nm profile are due to the random distribution of nodes in the polymer representation. If a uniform distribution of nodes were adopted the profiles would exhibit a smoother and more consistent plateau regime. For example, Fig. 16 depicts the pull-out profiles for three different lengths when using the polymer representation of Study 1. As can be seen the pull-out profiles show very little variability and the maximum pull-out force is identical for all three lengths. Therefore, it can be inferred that the maximum pull-out force remains relatively unchanged for CNTs of different lengths. This can be explained by reference to stress distributions in traditional fiber pull-out tests. It is well known that for the case of a continuous fiber composite with a load applied in the fiber direction there exist both normal and interfacial shear stresses. However, the distribution of these stresses differs along the embedded length of the fiber. The normal stresses vary linearly from a maximum at the loaded end of the fiber to zero at the embedded fiber end. The interfacial shear stresses, on the other hand, rise exponentially and peak at either the loaded or embedded ends depending on the material properties of the constituent materials (Fu et al., 1993). A similar interfacial shear stress distribution is observed in the present nanotube pull-out simulation. At the nanoscale, only vdW interactions participating with CNT atoms near the loaded end of the nanotube contribute to counteract the applied pull-out force. A two-dimensional schematic depiction of the vdW interactions at the interface is provided in Fig. 17. The vdW interactions acting on CNT atoms along the length of the nanotube have no cumulative effect on the pull-out force and ISS. Instead, the cumulative resultant vdW force is normal to the longitudinal axis of the nanotube and hence to the direction of nanotube loading. In comparison, the CNT atoms near the end of the nanotube have a component of the cumulative force opposing the pull-out force which contributes to the ISS. Therefore, increasing the CNT embedded length has no effect on the maximum pull-out force of non-bonded nanotubes; rather it only serves to extend the sliding regime of the pull-out profile, as depicted in Fig. 15.

Given that the maximum pull-out force is not affected by the CNT length, it is possible to examine its influence on the ISS simply by dividing the maximum force by the interfacial area for varied CNT lengths. The ISS of the CNT polymer composite system exhibits a decaying length dependence similar to traditional fiber composites, as shown in Fig. 18. This result allows one to extrapolate ISS values for CNTs of longer lengths that are too large to model due to the number of degrees of freedom involved. For example, if we were to consider an embedded CNT length of 100 nm the results predict an ISS of 1.45 MPa for the corresponding CNT polymer composite system.

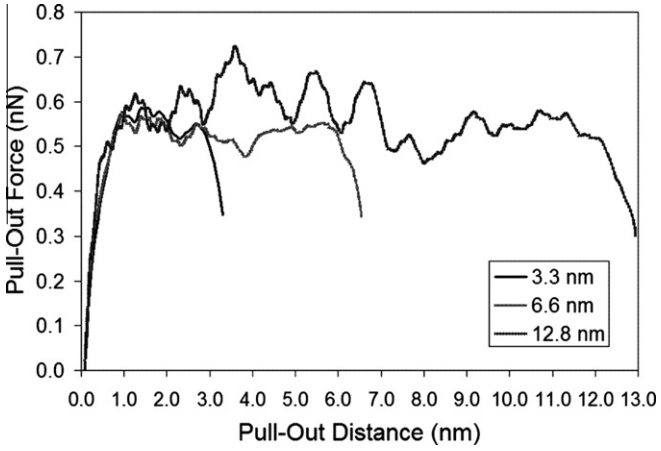

Fig. 15. Pull-out profiles for CNTs with different embedded lengths in the two-component epoxy formulation.

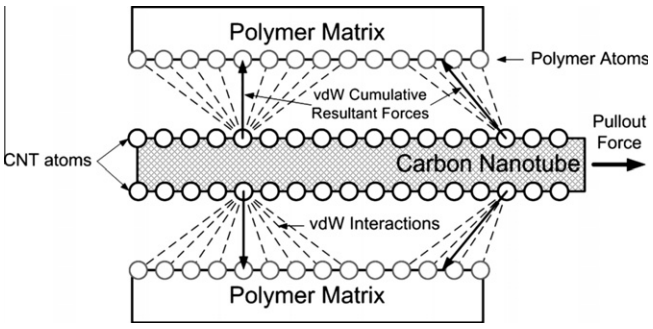

Fig. 17. Two dimensional schematic depiction of the cumulative resultant vdW forces along the length of a CNT during the pull-out process.

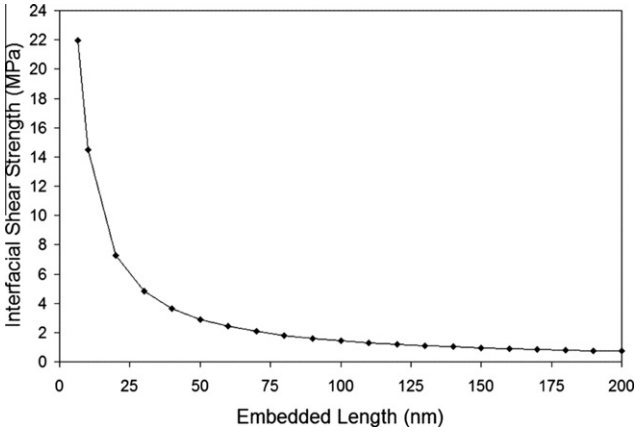

Fig. 18. Effect of embedded nanotube length on the interfacial shear strength.

3.3. Effect of interfacial thickness

A number of approaches have been considered to account for the interfacial properties of CNT polymer composites. These depend on the type of bonding, type of polymer matrix, and load transfer mechanisms considered. Hence, the interfacial thickness has not yet been unambiguously defined. Several different values have been used in both atomistic and continuum simulations. Hu et al. (2005) simulated the helical wrapping of one polystyrene chain around a CNT considering only van der Waals interactions via molecular dynamics. The equilibrium distance between the hydrogen atoms in the polymer and carbon atoms in the nanotube ranged from 0.2851 to 0.5445 nm. However, only one polymer chain was considered, while in practical cases there may be other chains which also wrap around the nanotube. In comparison, Li and Chou (2006) studied the compressive behavior of CNT/polymer composites and assumed that the inside surface of the polymer matrix was located at the same position as the outside surface of the nanotube, giving an interfacial thickness equal to 0.17 nm or half the thickness of the nanotube itself. Montazeri and Naghdabadi (2008) used an interfacial thickness of 0.3816 nm in their molecular structural mechanics model of SWCNT-polymer composites. This value corresponds to the equilibrium distance of the Lennard-Jones potential. Given the above variance, it is worthwhile to investigate the effect of different interfacial thicknesses on the ISS of the CNT polymer composite system.

Fig. 19 shows the predicted ISS for the two-component epoxy system over an interfacial thickness range of 0.30–0.46 nm for a CNT of 3.30 nm in length. An immediate observation is that the ISS increases with decreasing interfacial thickness. The present analysis adopts a constant computational volume that extends a radial distance of 1.0 nm from the wall of the CNT. As the interfacial thickness is decreased, a larger number of polymer atoms are included in the computational cell which increases the number of vdW interactions occurring over the interface and the subsequent ISS.

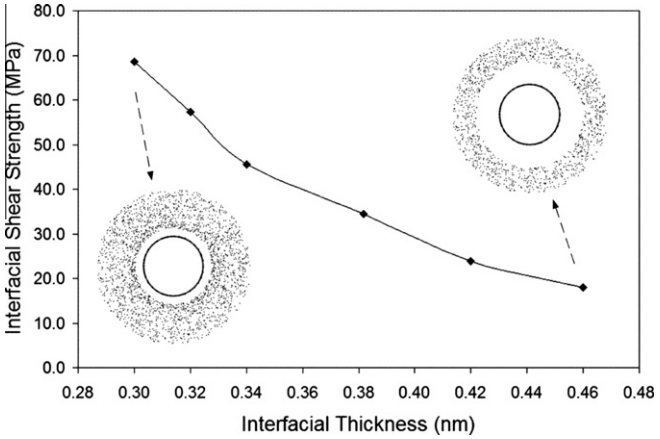

Fig. 19. Effect of interface thickness on the interfacial shear strength.

3.4. Effect of Lennard-Jones cut-off distance

In most MD approaches, the LJ interatomic potential used to simulate vdW interactions is often truncated to reduce computational cost so that atom pairs whose distances are greater than the truncation distance have a vdW interaction energy of zero. The truncation distance or cut-off distance is often taken to be 2.5ψ or 0.85 nm. At 2.5ψ, the LJ potential is approximately 1/60th of its minimum value. However, truncating the potential introduces a sharp discontinuity between atoms inside and atoms outside the cut-off radius, particularly when smaller cut-off distances are used. In the present study, vdW interactions dominate the solution and truncation of the LJ potential even at 2.5ψ can potentially introduce significant errors. Fig. 20 shows the calculated results for a cut-off range of 0.51 nm (1.5ψ) to 1.36 nm (4.0ψ) using an interfacial thickness of 0.34 nm and a CNT length of 3.3 nm. The dotted line in the figure is the predicted ISS when no cut-off distance is used and the LJ potential has an infinite range representing the true solution for this particular configuration. The associated error with each data point is provided in Table 4. As the cut-off distance is increased, the associated error decreases. At the traditional cut-off distance of 2.5ψ or 0.85 nm the solution still shows an error of approximately 25.71% suggesting that a cut-off distance of 3.5ψ (~7.91% error) would be more appropriate for this particular system. It should be noted that in all the above analyses no cut-off distance was incorporated.

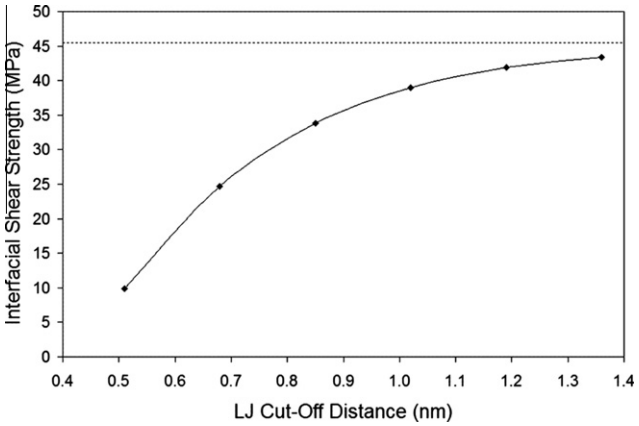

Fig. 20. Effect of LJ cut-off distance on the interfacial shear strength.

Table 4
Associated error in predicted ISS due to truncation of LJ potential.

Cut-off distance (nm)	τ_{ISS} (MPa)	Error (%)
0.51 (1.5ψ)	9.9	78.35
0.68 (2.0ψ)	24.7	45.71
0.85 (2.5ψ)	33.8	25.71
1.02 (3.0ψ)	39.0	14.29
1.19 (3.5ψ)	41.9	7.91
1.36 (4.0ψ)	43.4	4.62
Infinite	45.5	0.00

3.5. Effect of CNT diameter

The use of CNTs as reinforcing agents in epoxies allows for nanotubes with various diameter ranges to be selected. The diameter of a CNT can have an effect on its macroscopic reinforcement properties, which needs to be understood. Here, we examine five nanotubes of length 4.2 nm embedded in the two-component DGEBA/TETA polymer representation. Armchair configurations are considered, with the smallest being a (5,5) nanotube, and the largest an (18,18) nanotube. In order to minimize the effect of polymer distribution on the pull-out curves, an identical polymer configuration is used for all simulations, and polymer atoms outside the 0.34–1.34 nm interfacial range are deleted after modeling the nanotube. Fig. 21 shows the pull-out profiles predicted for CNTs of different diameters while Fig. 22 illustrates the approximately linear dependence of the ISS on the CNT diameter. However, as the diameter increases, the ISS decreases until it plateaus at approximately 25.9 MPa. This reduction demonstrates the advantage of using small diameter SWCNTs, due to their significantly higher ISS values when compared to larger diameter CNTs. The results of this study are summarized in Table 5.

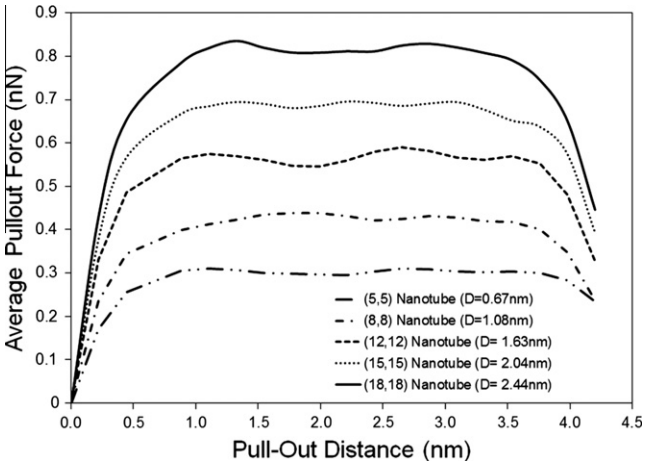

Fig. 21. Pull-out profiles for CNTs of varying diameter.

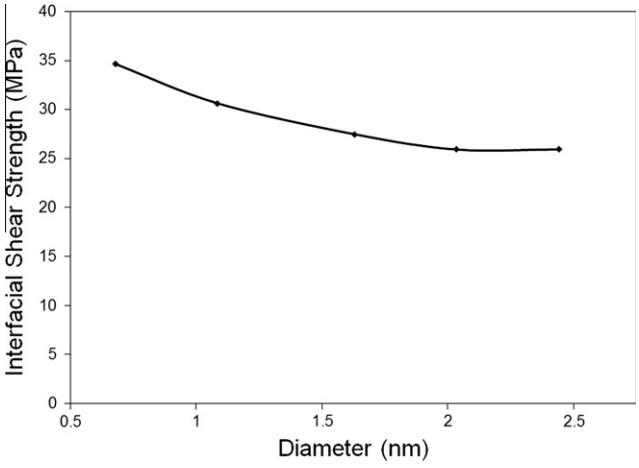

Fig. 22. Effect of diameter on the interfacial shear strength.

3.6. Effect of CNT and polymer capping

The previous studies examined the key parameters that influence the ISS for a non-bonded pull-out configuration where the CNT extended the same distance as the surrounding polymer. In all these cases, the pull-out profiles did not exhibit the initial characteristic peak in the pull-out force that is evident in experimental pull-out profiles. In this section, we illustrate the importance of accounting for the vdW interactions that occur at the base of the embedded CNT by incorporating both CNT caps and a polymeric region below the CNT. From this point forward, we refer to the polymeric region below the CNT as a polymeric end-cap. In this case, we consider a (10,10) armchair nanotube of length 4.42 nm embedded in the two-component DGEBA/TETA epoxy polymer representation. Five different capping conditions are considered and are summarized in Table 6 along with their schematic representations in Fig. 23.

An un-conforming polymeric end-cap refers to the case when the CNT is capped and the surrounding polymer does not entirely conform to its contour (Condition D). The interfacial thickness is slightly larger than the constant value of 0.34 nm used in our previous simulations near the base of the CNT. One should also note that the capped CNT geometries are offset from the uncapped geometries by a distance of approximately 0.27 nm. This is due to the curved shape of the CNT cap, which in turn reduces the effective length of the CNT. The tight polymeric end-cap condition does conform to the CNTs capped contour (Condition E). The polymer matrix entirely surrounds the CNT with a constant interfacial thickness of 0.34 nm. The most notable difference between these two scenarios is that the magnitudes of the vdW forces acting at the base of the CNT in the un-conforming condition are reduced due to the larger separation distances between the polymer and CNT atoms.

An initial comparison of the pull-out profiles for all five capping conditions is shown in Fig. 24. Examining the pull-out profiles highlights the significant effect that the capping condition can have on the pull-out characteristics. The most notable difference is the initial peaks evident in the pull-out profiles for Conditions B and E. These peaks arise from the added vdW interactions between the polymer and CNT atoms at the base of the nanotube when considering tight polymeric end-caps. Fig. 25 illustrates the additional vdW forces that arise from these capping conditions which appose the applied pull-out force. A capped CNT with a tight polymeric end-cap (Condition E) has a peak pull-out force 2.85 times larger than the base condition A where neither a CNT cap nor a polymeric end-cap were considered. This results in a 16% increase in the energy required to pull out the CNT from the surrounding polymer (for a 4.42 nm CNT). The additional vdW interactions that arise from the added CNT and polymer atoms significantly improve

Table 5
Details of the capping conditions considered.

Capping scenario	CNT structure	Polymer end condition
A	(10,10) Uncapped	No polymeric end-cap
B	(10,10) Uncapped	Polymeric end-cap
C	(10,10) Capped	No polymeric end-cap
D	(10,10) Capped	Un-conforming polymeric end-cap
E	(10,10) Capped	Tight polymeric end-cap

Table 6
Pull-out results with varying nanotube diameters.

CNT chirality	CNT diameter (nm)	Peak pull-out force (nN)	τ_{ISS} (MPa)
(5,5)	0.678	0.310	34.656
(8,8)	1.085	0.439	30.631
(12,12)	1.628	0.590	27.474
(15,15)	2.035	0.696	25.907
(18,18)	2.443	0.835	25.924

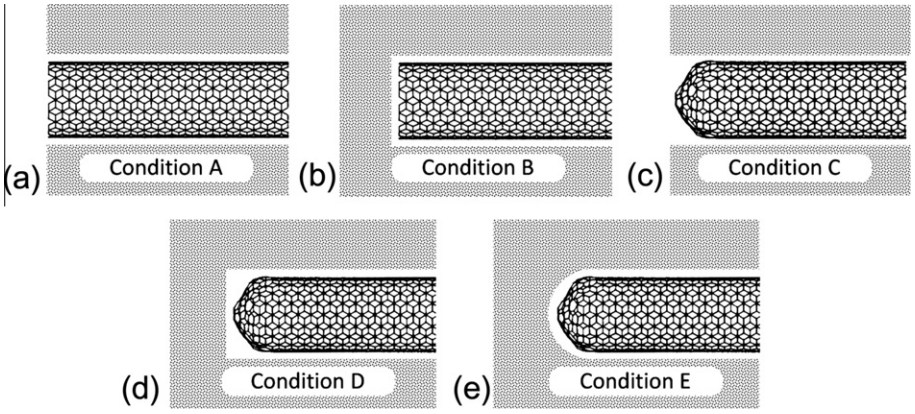

Fig. 23. Different capping conditions considered.

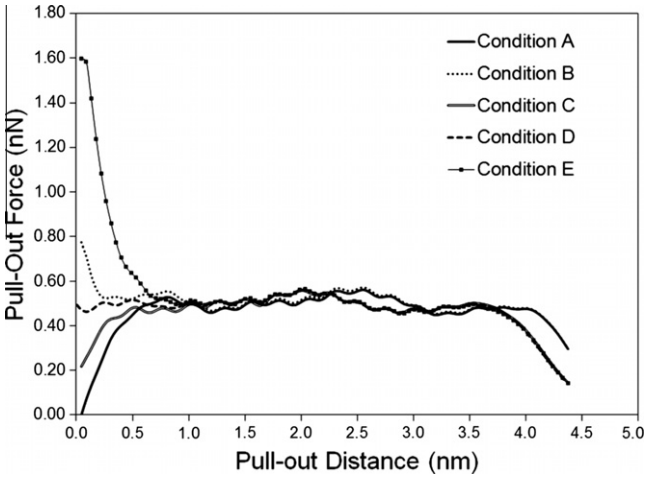

Fig. 24. Pull-out profiles for capping conditions A through E.

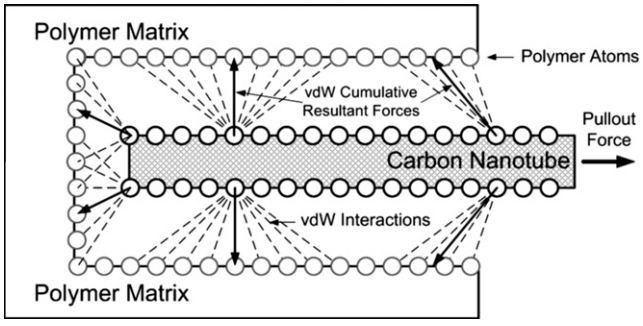

Fig. 25. Two dimensional schematic depiction of the cumulative resultant vdW forces along the length and base of a CNT during the pull-out process.

the peak pull-out force and produce profiles characteristic of those observed in experiments. One might expect a similar result for Condition D, however, the peak pull-out force for this condition deviates by only 0.09% from the baseline condition. This is due to the larger interfacial thickness near the base which serves to reduce the magnitude of the vdW forces in that region. In addition, the capped CNT with no polymeric end-cap (Condition C) does not seem to deviate much from the baseline. As such, we can conclude that CNT caps do not significantly affect the magnitude of the pull-out force unless fully surrounded by the polymer matrix such that the additional atoms are capable of participating in these interactions. A summary of the pull-out results for each condition is provided in Table 7.

4. Conclusions

A nanotube pull-out test has been simulated using the ABC multiscale modeling technique to investigate the interfacial properties of CNT polymer composites. Only vdW interactions were considered between the atoms in the CNT and the polymer implying a non-bonded system. The vdW interactions were simulated using the LJ potential, while the CNT was described using the Modified Morse potential. The results reveal that the ISS shows a linear dependence on the vdW interaction density and decays significantly with increasing nanotube embedded length. The thickness of the interface was also varied and our results reveal that lower interfacial thicknesses favor higher ISS. When incorporating a 2.5ψ cut-off distance to the LJ potential, the predicted ISS shows an error of approximately 25.7% relative to a solution incorporating an infinite cut-off distance. Increasing the diameter of the CNT was found to increase the peak pull-out force approximately linearly. Finally, an examination of polymeric and CNT capping conditions showed that incorporating an end cap in the simulation yielded high initial pull-out peaks that better correlate with experimental findings. These findings have a direct bearing on the design and fabrication of carbon nanotube reinforced epoxy composites.

Table 7
Pull-out results for different capping conditions.

Capping condition	Peak pull-out force		Average steady-state pull-out force		Pull-out energy	
	(N)	(% Change)	(N)	(% Change)	(nJ)	(% Change)
A	5.61E−10	–	5.06E−10	–	2.02E−09	–
B	7.73E−10	37.81%	5.14E−10	1.52%	2.22E−09	9.51%
C	5.57E−10	−0.72%	5.09E−10	0.60%	2.00E−09	−1.05%
D	5.61E−10	0.09%	5.11E−10	0.93%	2.07E−09	2.19%
E	1.60E−09	184.83%	5.10E−10	0.63%	2.36E−09	16.36%

Acknowledgements

The authors wish to acknowledge the financial support provided by the Natural Sciences and Engineering Research Council of Canada (NSERC).

References

Barber, A.H., Cohen, S.R., Wagner, H.D., 2003. Measurement of carbon nanotube-polymer interfacial strength. Appl. Phys. Lett. 82, 4140–4142.

Barber, A.H., Cohen, S.R., Eitan, A., Schadler, L.S., Wagner, H.D., 2006. Fracture transitions at a carbon-nanotube/polymer interface. Adv. Mater. 18, 83–87.

Belytschko, T., Xiao, S.P., Schatz, G.C., Ruoff, R.S., 2002. Atomistic simulations of nanotube fracture. Phys. Rev. B 65, 235430–1-8.

Cooper, C.A., Cohen, S.R., Barber, A.H., Wagner, H.D., 2002. Detachment of nanotubes from a polymer matrix. Appl. Phys. Lett. 81, 3873–3875.

Endo, M., Hayashi, T., Kim, Y.A., Terrones, M., Dresselhaus, M.S., 2004. Applications of carbon nanotubes in the twenty-first century. Phil. Trans. R. Soc. Lond. A 362, 2223–2238.

Fiedler, B., Gojny, F.H., Wichmann, M.H.G., Nolte, M.C.M., Schulte, K., 2006. Fundamental aspects of nano-reinforced composites. Compos. Sci. Technol. 66, 3115–3125.

Frankland, S.J.V., Caglar, A., Brenner, D.W., Griebel, M., 2002. Molecular simulation of the influence of chemical cross-links on the shear strength of carbon nanotube-polymer interfaces. J. Phys. Chem. B 106, 3046–3048.

Fu, S.Y., Zhou, B.L., Chen, X., Xu, C.F., He, G.H., Lung, C.W., 1993. Some further considerations of the theory of fibre debonding and pull-out from an elastic matrix, I - constant interfacial frictional shear stress. Compos. 24, 5–11.

Garg, A., Sinnott, S.B., 1998. Molecular dynamics simulations of the filling and decorating of carbon nanotubules. Chem. Phys. Lett. 295, 273–277.

Hu, N., Fukunaga, N., Lu, C., Kameyama, M., Yan, M., 2005. Prediction of elastic properties of carbon nanotube reinforced composites. Proc. R. Soc. Lond. A 461, 1685–1710.

Hu, Y., Shenderova, O.A., Zushou, H., Padgett, C.W., Brenner, D.W., 2006. Carbon nanostructures for advanced composites. Rep. Prog. Phys. 69, 1847–1895.

Iijima, S., 1991. Helical microtubules of graphite carbon. Nature 354, 56–58.

Li, C.Y., Chou, T.S., 2006. Multiscale modeling of compressive behavior of carbon nanotube/polymer composites. Compos. Sci. Technol. 66, 2409–2414.

Mader, E., Jacobasch, K., Grundke, K., Gietzelt, T., 1996. Influence of an optimized interphase on the properties of polypropylene/glass fibre composites. Compos.: Part A 27, 907–912.

Montazeri, A., Naghdabadi, R., 2008. Investigation the stability of SWCNT-polymer composites in the presence of CNT geometrical defects using multiscale modeling. Proceedings of the Fourth International Conference on Multiscale Materials Modeling, 163–166.

Wagner, H.D., Laurie, O., Feldman, Y., Tenne, R., 1998. Stress-induced fragmentation of multiwall carbon nanotubes in a polymer matrix. Appl. Phys. Lett. 72, 188–191.

Wernik, J.M., Meguid, S.A., 2011. Multiscale modeling of the nonlinear response of nano-reinforced polymers. Acta Mech. 217, 1–16.

Xia Z., Curtin, W.A., 2004. Pullout forces and friction in multiwall carbon nanotubes. Phys. Rev. B 69, 233408-1-4.

Xu, X., Thwe, M.M., Shearwood, C., Liao, K., 2002. Mechanical properties and interfacial characteristics of carbon-nanotube-reinforced epoxy thin films. Appl. Phys. Lett. 81, 2833–2836.

Zheng, Q., Xia, D., Xue, Q., Yan, K., Gao, X., Li, Q., 2009. Computational analysis of effect of modification on the interfacial characteristics of a carbon nanotube-polyethylene composite system. Appl. Surf. Sci. 255, 3534–3543.